Experimental analysis of two-phase flow in domestic central heating systems: micro bubble characteristics

A. M. Fsadni[1], Y. T. Ge[1] & A. G. Lamers[2]
[1]*Department of Mechanical Engineering, Brunel University, UK*
[2]*Spirotech bv, The Netherlands*

Abstract

Domestic central heating systems result in micro bubble nucleation and detachment at the boiler wall due to the presence of supersaturated conditions in the system. Such conditions originate due to the widespread use of untreated tap water in such systems and due to the air leakage into the system's closed loop circuit during the daily thermal cycling. The presence of air bubbles in such systems results in a number of undesired effects such as corrosion, blockages, noise and the filling of radiators with air due to the deposit of the micro bubbles in the radiators. As a result, a loss in the heat transfer area of the radiator occurs thus resulting in an inefficient use, consequently increasing the carbon footprint of such widely used systems. Therefore, the capture of micro bubbles at the exit point of the boiler should result in improved system efficiencies. A comprehensive knowledge of the expected bubble production rate and bubble size is important for an efficient deaeration system. To date, no studies have been published on the fundamentals of bubble production and size in wet central heating systems, therefore, the importance of this paper for the building services industry. Experimental results on a test rig incorporating a typical 19 kW (rated) domestic gas fired boiler show typical micro bubble production rates ranging between 0.03 to 0.47 litres of nitrogen gas per hour with a shift in the system heating load. An analysis of the expected bubble diameters was done at different system conditions. Bubbles with average diameters within the range of 0.13 and 0.39 mm were observed. A comparison with Winterton's finite angle force balance model resulted in reasonable predictions.
Keywords: micro bubbles, supersaturated solutions, central heating, dissolved gasses, space heating.

WIT Transactions on Engineering Sciences, Vol 70, © 2011 WIT Press
www.witpress.com, ISSN 1743-3533 (on-line)
doi:10.2495/MPF110141

1 Introduction

Micro bubble formation is a phenomenon affecting a number of industries, including the food, pharmaceutical, building and chemical industries. Bubble nucleation finds its origins in the presence of superheated or supersaturated solutions. In a domestic central heating system micro bubble formation is the result of water supersaturated with dissolved nitrogen gas, consequently, leading to bubble nucleation on the boiler wall. The use of the term boiler for a standard domestic central heating unit could suggest that some form of boiling takes place in the system's primary heat exchanger, consequently leading to the formation of bubbles through superheat. However, under no operating conditions does the phenomenon of flow boiling or sub cooled flow boiling take place in a domestic central heating unit. This is necessary so as to avoid excess noise originating from the boiler unit and to prevent excessively high exit temperatures thus ensuring the safe operation of the system within the domestic environment.

Micro bubble nucleation is solely attributed to the presence of gas super saturation levels in the water flowing in the system's closed loop circuit. Long term tests have shown that such systems could result in saturation ratios as high as 1.2 at the boiler wall conditions. Such conditions are present during cold start-ups and after the system filling with tap water. Air is mostly absorbed in the system during the cold cycle. At low temperatures, water can absorb the highest quantity of dissolved gasses [1, 2]. In most systems this occurs during night time when the system's boiler shuts off.

Data on micro bubble characteristics in central heating systems is important as a good knowledge of bubble sizes and their distribution is essential for an efficient passive deaeration process. Passive deaerators are more efficient in capturing larger sized bubbles. Deaeration is an important feature of such systems as bubbles accumulate in radiators and result in cold spots, thus reducing the heat transfer area of the radiator and the overall system efficiency. Bubbles are also known to result in unwanted noise, blockages and corrosion. Domestic central heating systems amount to 16% of the carbon dioxide emissions in the UK [3] and consequently an optimised system performance should have significant environmental benefits. The widespread use of domestic central heating systems was also highlighted by Spreitzer *et al.* [4] who state that almost all residential buildings in Germany make use of a wet central heating system which results in circa 40% of the primary energy consumed in Germany. Furthermore, Sauer *et al.* [5] also state that central heating systems are responsible for 70% of all domestic emissions in Germany.

A bubbly flow in the circuit's forward flow line results from the detachment of micro bubbles from the boiler wall into the system. Bubbly two-phase flow is characterised by the presence of bubbles of maximum size much less than the containing vessel or duct. The bubbles are dispersed in a continuous liquid phase [6]. From our test results no micro bubbles were observed on the return line to the boiler, thus suggesting that micro bubbles dissolve, are deaerated or rise to high points in radiators or vessels while flowing through the system. The analogy between this present study and theories developed for the prediction of bubble

diameters in two-phase fully developed turbulent bubbly flow in ducts extended this study to the consideration of the two known models for predicting bubble sizes, these being the Hinze [7] approach as adapted by Winterton and Munaweera [6], and the Winterton and Orby [8] approach. However, these studies are based on experimental data obtained through the artificial insertion of micro bubbles in the flow.

In this paper we will investigate the phenomenon of micro bubbles in wet domestic central heating systems. The average bubble diameters, size distributions and bubble production rates at typical primary heat exchanger saturation ratios will be investigated.

2 Theory

2.1 The solubility of gasses in liquids and supersaturated solutions

Fogg [9] states that the solubility of gases in a liquid is a property of a gas dependent on its partial pressure and on the temperature as well as the nature of the liquid phase. In fact, for most gas-liquid systems there tends to be a linear variation of solubility with the partial pressure as this approaches zero. When defining the solubility of gases, Young *et al.* [2] highlight the point that the distinction between vapor-liquid equilibria and the solubility of gases in liquids is arbitrary and often the distinction between the two is not clear. This issue arises from the general inability to rigorously distinguish between a gas, a vapor and a liquid. However, Gerrard [1] defines gases as all the elements and compounds having a boiling point at 1 atm less than 13°C. Gas solubility data at standard atmospheric and volumetric conditions is available through a number of publications [2].

Jones *et al.* [10] defines a supersaturated solution in relation to quantifying the tendency of a system to produce bubbles. They refer to the saturation data as a function of the temperature for the system. A solution could go into the supersaturated state through the increase of its temperature. In fact, point A in fig. 1 represents a saturated solution at a temperature T_A with a saturation mole fraction amounting to X_b. When the temperature of this solution is increased to T_B, the solution would be in its supersaturated state while still retaining the previous mole fraction of the dissolved gas content. The desorption of gas from the water then causes the state of the system to move gradually from point B to point B' with a new saturation mole fraction equal to X_i. In view of this the resultant saturation ratio is defined through the relationship in eqn. (1);

$$\alpha = \frac{X_b}{X_i} \tag{1}$$

Furthermore, the super saturation ratio is defined as

$$\sigma = \alpha - 1 \tag{2}$$

Our saturation ratio was calculated through the use of eqns. (3) and (4). as done by Lubetkin and Blackwell [11] who calculated the gas concentration in the fluid through the use of the Henry's law as defined by Gerrard [1]. The partial gas pressure was calculated by subtracting the vapour pressure from the total dissolved gas pressure.

$$C_{gas} = P_g X^T \tag{3}$$

The saturation ratio was calculated through the use of eqn. (1). As shown in eqn. (4), the ratio of the actual gas concentrations was used where C_{sat} refers to the maximum gas solubility at the primary heat exchanger wall temperature.

$$\alpha = \frac{C_{gas}}{C_{sat}} \tag{4}$$

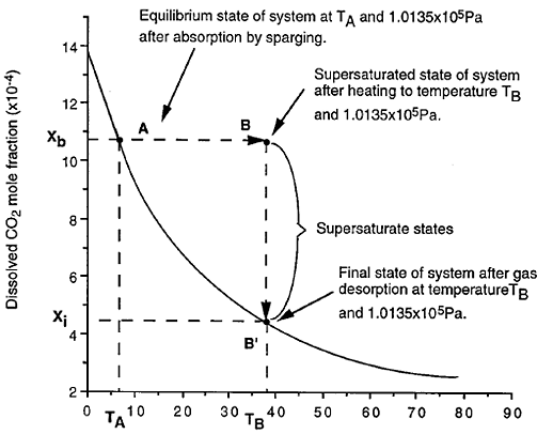

Figure 1: Solubility of carbon dioxide [10, p.30].

2.2 Bubble size prediction

Research in bubble nucleation and growth in supersaturated solutions is not widespread and consequently the number of studies available is limited to very specific and theoretical systems. A model for predicting the detachment radius of bubbles originating in supersaturated duct flow is based on the balance of the drag and surface tension forces acting on the surface of the nucleating bubble on the primary heat exchanger wall, parallel to the wall surface. Winterton's [12] approach for the prediction of bubble detachment diameters is based on this theory. Other models have been developed for predicting the bubble radii such as the approach originally suggested by Scriven [13] and later adapted by Jones *et al.* [10]. These models are based on the symmetric phase growth controlled by heat and mass transfer.

These models were developed for modelling bubble nucleation and require a comprehensive knowledge of the surface conditions and the bubble nucleating time. The lack of knowledge with respect to the bubble nucleating time in the helical coils of the boiler's primary heat exchanger made this model unusable in the present study. The model developed by Winterton [12] is based on the knowledge that bubbles break away from the surface into the flow when the drag force equals the surface tension force. For a finite contact angle Winterton [12] derived eqn. (5) for the experimental conditions of the present study.

$$\frac{r}{R_h} = 1.4\left[\frac{F(\theta)}{We}\right]\mathrm{Re}^{0.24} \tag{5}$$

where $F(\theta) = \sin\theta_0(\cos\theta_r - \cos\theta_a)$ and $We = \frac{(\rho u^2 D_h)}{\gamma}$.

A number of recent studies have adapted the use of the Winterton model with good results. Amongst these are studies done by Al-Hayes and Winterton [14, 15] and Hepworth *et al.* [16]. Al Hayes and Winterton adapted the original Winterton model to include the effect of liquid motion on the bubble growth rate due to the change in the mass transfer coefficient for the gas entering the bubble from the bulk liquid. Their final approach is similar to the original Scriven [13] and Jones *et al.* [10] models and thus requires a comprehensive knowledge of the bubble nucleating time.

3 Experimental facility

A schematic diagram of the experimental set up is shown in fig. 2. The test rig consists of a Valliant eco TEC pro 24 condensing boiler that is connected to standard 22mm copper tubing which supplies a radiator and a buffer vessel. A condensing boiler is used as this is mandatory equipment for new buildings in most European Union member states [3]. Stainless steel sheathed K type thermocouples are used to measure the fluid temperatures along the circuit whereas pressure transducers monitor the system pressure. A pressure transducer monitors the dissolved gas partial pressure in combination with a semi permeable silicone membrane. The system fluid flow rate is monitored through an Electromag 500 Series electromagnetic flow meter. A National Instruments cDAQ-9172 chassis and data modules receive all the signals from the transducers, thermocouples and the electromagnetic flow meter. The three system parameters are controlled as follows:

i The system flow rate or velocity is varied through the use of a ball valve on the supply line. The velocity in the boiler tubes was stepped between a minimum 0.3 m/s and a maximum of 0.8 m/s. This is equal to a system flow rate ranging from 4.5 to 12.5 litres per minute. The system pressure was set at 2.75 bars with a saturation ratio of 1.1 at the boiler wall conditions.

ii The system heating load was varied between a minimum of 7.5 kW and a maximum of 21.5 kW through the step increase in the boiler flame settings. The heating load is equal to a boiler heat flux ranging between 17 and 50 kW/m^2. The

inlet temperature was maintained at a constant 55°C to ensure sufficient latent heat recovery through the boiler in-built condenser. The exit temperature ranged between 65 and 84°C while a system pressure of 2.75 bars (abs) was maintained. An average saturation ratio of 1.1 at the boiler wall conditions was maintained.

iii Super saturation ratios, ranging between 1 and 1.2 at boiler wall conditions were achieved through the filling of the top part of the radiator with nitrogen gas. The system pressure was set at 2.75 bars and a system flow rate of 12.5 litres per minute was maintained.

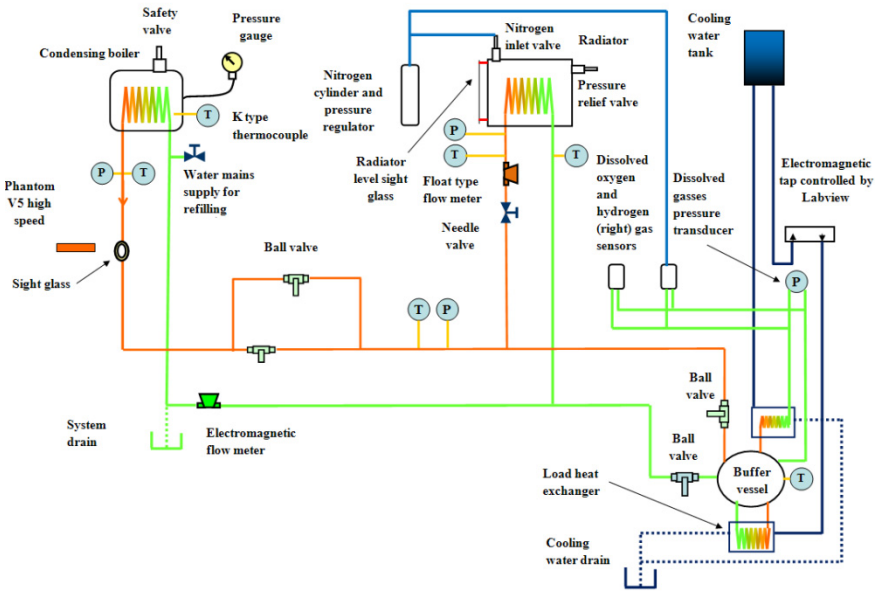

Figure 2: Schematic diagram of experimental set up.

Standard central heating systems make use of untreated steel radiators and copper piping. The untreated radiators result in a limited amount of oxidation due to the dissolved oxygen present in the tap water. The oxidation process releases iron oxide and some hydrogen gas. The analysis of dissolved gases through the use of Orbisphere 3655 oxygen and Orbisphere 3654 hydrogen sensors resulted in very low concentrations of oxygen and hydrogen present in their dissolved form. In fact both gases were present in concentrations of circa 9 PPB. Therefore, nitrogen is evidently the dominant gas and its properties were used for the dissolved gas properties in this study. A square sight glass with internal dimensions of 20x20 mm was used for filming micro bubbles at the exit line of the boiler. A square section was designed to reduce the distortion as a result of viewing bubbles through a curved surface. As discussed by Prodanovic *et al.* [17], such distortions are due to light refraction. A Vision research Phantom V5 high speed camera connected to a PC was used to film and store the video clips. A monozoom (Navitar) microscope lens was used to develop the

desired magnification and a shutter speed of 30 μs and a frame speed of 100 frames per second were used. Lighting was provided by two high intensity Everest.VIT ELSV 60 W light sources attached to semi rigid fibre optic light guides.

4 Image analysis

The video films were converted to image frames saved as 'tag image file format' or tiff files using the Phantom Version 606 camera software. The analysis of the bubble diameters was done manually using the Phantom Version 606 Image Analysis software using a representative sample of 100 bubbles for each experimental run [17]. This was done so as to ensure an accurate result due to the general limitations of the automated image processing software.

The bubble production rates were calculated through the use of the image analysis software, Image-Pro Plus developed by Media Cybernetics. An average of 1500 frames were analysed for each experimental run. A macro was written enabling a series of images to be analysed for in focus bubble counts and diameters. The macro included the use of a Sobel filter to enable the distinction between in and out of focus bubbles. The Sobel filter plots the gradient of intensity change between objects and their background through the extraction and enhancement of edges and contours. This is done by expressing intensity differences or gradients between neighbouring pixels as an intensity value. Therefore, objects that are in focus have sharp edges with a high gradient change and consequently result in a high intensity values, whereas out of focus objects do not display such a characteristic. The Sobel filter was used as it is less sensitive to image noise when compared to other filtering techniques [18]. A typical analysed image is illustrated in fig. 3, where in focus bubbles are circled. Experimental uncertainties were calculated based on the method given by Coleman and Steel [19] and estimated as a mean absolute value of 3% for the manual bubble diameter measurements and 12% for the bubble production rates.

5 Results and discussion

The measured bubble diameters are illustrated in fig. 4. These measurements have shown an increase in the bubble diameter with an increase in heat flux or

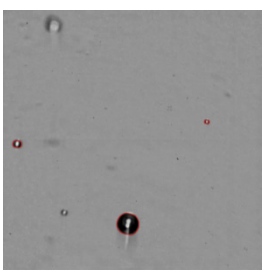

Figure 3: Camera image (post processing – in focus bubbles circled).

the corresponding space heating load and a decrease in velocity. Changes in the super saturation ratios did not result in notable bubble diameter differences. Bubbles were mostly spherical in shape and therefore, no elongation is attributed to the surrounding fluid flow. This is in agreement with recent studies done in bubbly flows [6]. The present study did not permit a real time measurement of the bubble diameters during their detachment from the heat exchanger wall. Therefore, the positioning of the sight glass at the exit end of the boiler with sufficient insulation to ensure adiabatic bulk fluid flow conditions, allowed the authors of the present study to assume that the observed bubble diameters are reasonably equal to the detachment diameters. Furthermore, the effects of bubble coalescence and dissolution during their short time in the bulk fluid flow were assumed to be at a minimum.

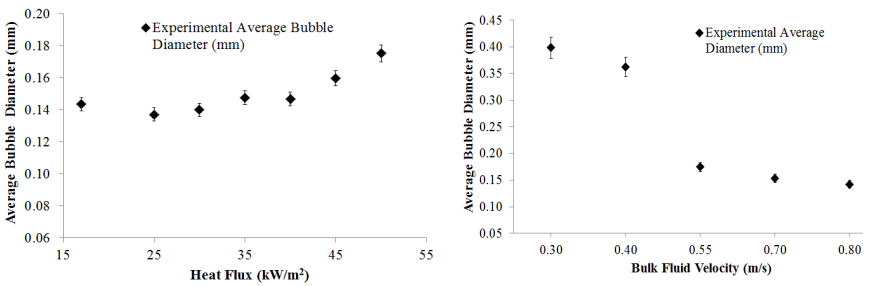

Figure 4: Average bubble diameters with heat flux and velocity in heating tubes.

Winterton's finite contact angle model predicts the bubble diameters with changing system parameters with a mean absolute error of 20%.As illustrated in fig. 5, all data points fall between ± 30% of the model prediction. With due consideration to the limitations of studies in two-phase flow as discussed by Winterton and Munaweera [6] and the general limitations of the present study, the adapted model predicts the expected bubble diameters reasonably well. The Winterton model accurately predicts the decrease in bubble diameter with an increase in bulk fluid velocity for velocities ranging from 0.4 to 0.8 m/s. However, at a lower velocity the error amounted to 45%. The inclusion of the Weber and Reynolds number enables the Winterton model to predict the bubble detachment diameters with changing bulk fluid flow. Similar experimental results were observed by Al-Hayes and Winterton [14] and in studies done in sub cooled flow boiling by Prodanovic *et al*. [17]. Other more recent studies done by Hepworth *et al.* [16] suggest that the bulk fluid velocity could increase the bubble growth rate and consequently lead to higher nucleation rates due to the liquid motion affecting the mass transfer coefficient for the gas entering the bubble on the heat exchanger wall. As illustrated in fig. 4, the increase in heat flux resulted in an increase in the bubble diameter by circa 20%. This is attributed to the higher boiler wall temperatures resulting in an increase in the diffusivity of nitrogen moving into the bubbles growing on the heat exchanger

wall. This trend is not well represented in the Winterton finite contact angle force balance model. However, a minimal increase in the predicted diameter is represented through the change in the fluid properties, such as the density, kinematic viscosity and surface tension. Jones *et al.* [10] predict a reduced nucleation time with higher temperature due to the higher diffusivities present at the heat exchanger wall. However, this is not reflected on the predicted bubble detachment diameter. Similar trends were reported by Abdelmessih *et al*. [20] in flow boiling.

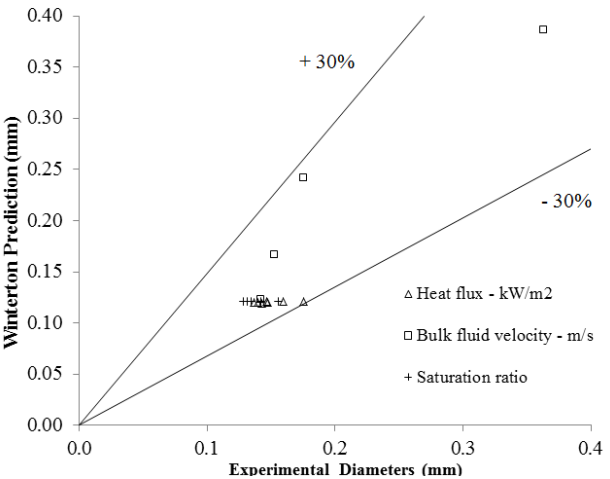

Figure 5: Accuracy plot.

Changes in the saturation ratio did not result in notable differences in the bubble diameters. A higher gas concentration gradient at the boiler's primary heat exchanger wall is expected to result in an increase in the bubble growth rate. However, the force balance theory seems to dominate and thus a minimal effect is seen on the resultant bubble diameter. Hepworth *et al.* [16] reported an increase in the bubble diameter with an increase in their dissolved gas concentration. However, higher saturation ratios were present and consequently, our observed constant bubble diameter with changes in the saturation ratio could be attributed to the narrow super saturation range present in our system.

The bubble distributions illustrated in fig. 6 illustrate the expected trends as seen in the experimental mean diameters whereby smaller bubbles make up a greater percentage of the total bubble count for the lower heat flux levels. Higher heat flux or heating loads could result in increased saturation ratios present at the boiler wall and therefore, a higher bubble production rate. However, the higher percentage of larger bubbles present at high system heating loads would facilitate the deaeration process through a passive deaerator and therefore at higher loads systems are expected to deaerate more efficiently. In fact, passive deaeration systems make use of deaeration chambers where bubbles float up a column where they are subsequently expelled through a float valve.

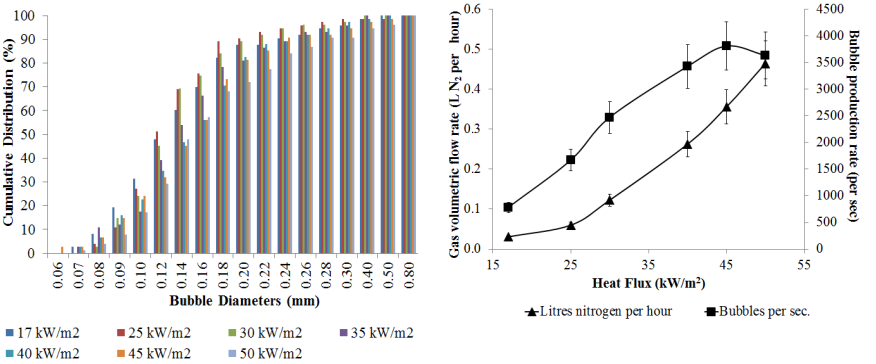

Figure 6: Bubble distribution, volumetric flow and production rate with heat flux.

Fig. 6 also illustrates the bubble production rate and the volume of air exiting the heat exchanger. The system bubble production rates range from 800 to 3800 bubbles per second. This corresponds to a gas volume production ranging from 0.03 to 0.46 litres per hour of operation at a constant system flow rate of 12.5 litres per minute. Tests have shown that the bubbles produced do not return to the boiler. Therefore, such bubbles are expected to dissolve back to the water in colder regions in the system or rise to high spots such as radiators located on the higher floors. Continuous system operation would therefore lead to the formation of a gas filled void at the top part of the radiators, consequently reducing the heat transfer efficiency, prompting the system user to increase the system operation time and exit temperature. This results in an increased carbon footprint. The system could then require the process of bleeding followed by a system re-pressurisation. No literature sources discussing bubble gas volumes in similar systems are known to exist. Therefore the possibility of data comparison here is very limited. However, when considering the total bubble production together with the boiler area that is under super saturation conditions, the average nucleation rate amounts to circa 1.3 bubbles/cm^2 s. This compares well with similar studies, most notably that done by Verschaeren on smooth metal heated surfaces [21].

6 Conclusions

This study has adapted mostly theoretical two-phase studies to more practical grounds that could lead to a better understanding of the two-phase characteristics in wet domestic central heating systems. An analysis of the expected micro bubble diameters has resulted in bubbles with average diameters within the range of 0.13 and 0.39 mm with changing system parameters. Good predictions were achieved through the use of Winterton's finite contact angle force balance prediction for bubble detachment radii in supersaturated solutions. Tests have shown that the average bubble diameter decreases with an increase in the bulk fluid velocity and a reduced heat flux and exit temperature while no change was

evident with changes in the saturation ratio. An analysis of the typical bubble size distribution over a range of heating loads and at a typical saturation ratio of 1.1 at the primary heat exchanger wall has shown a larger concentration of smaller sized bubbles at lower heat flux levels. The system bubble production rates ranged from 800 to 3800 bubbles per second while the corresponding gas volume production ranged from 0.03 to 0.46 litres of nitrogen gas per hour of operation at the minimum and maximum system heating loads respectively.

Acknowledgement

The authors would like to thank the Engineering and Physical Science Research Council, Spirotech b v., The Netherlands for supporting this research work.

Notation

C_{gas} Gas concentration in system, (standard cm^3/Litre Water)
C_{sat} Maximum gas concentration at boiler wall temperature, (standard cm^3/Litre Water)
D_h Helical tube hydraulic diameter, (m)
P_g Partial pressure of dissolved gas and vapour pressure, (Pa)
r Bubble detachment radius, (m)
R_h Helical tube hydraulic radius, (m)
Re Reynolds number, (-)
u Bulk fluid velocity, (m/s)
X_b Bulk gas concentration, (mol/m^3)
X_i Saturation gas concentration, (mol/m^3)
X_T Gas solubility factor, (standard cm3/Litre Water/bar)

Greek letters

α Saturation ratio, (-)
γ Surface tension, (N/m)
θ_a Advancing contact angle, (degrees)
θ_o Static contact angle, (degrees)
θ_r Receding contact angle, (degrees)
ν Kinematic Viscosity, (m^2/s)
ρ Water density, (kg/m^3)
σ Super saturation ratio, (-)

References

[1] Gerrard W., *Solubility of gases and liquids*, Plenum Press, New York, 1976.
[2] Young C.L., Battino R., Clever H.L., *The solubility of gases and liquids – introductory information, Nitrogen and Air, solubility data series – Volume 10*, Pergamon Press, Oxford, 1982.
[3] *The Building Regulations, Conservation of Fuel and Power – Part L1A*, Office of the Deputy Prime Minister, 2006.

[4] Spreitzer K., Rückbrodt D., Straky H., Observer-based estimation of the water mass flow through a central heating boiler, *Proceedings of the American Control Conference Anchorage AK*, **37,** pp. 5054-5059, 2002.
[5] Sauer J., Schmeink C., Wastell D.G., Feedback Quality and Environmentally Friendly Use of Domestic Central Heating Systems, *Journal of Ergonomics*, **50.(6)**, pp. 795-813, 2007.
[6] Winterton R.H.S., Munaweera J.S., *Bubble size in two-phase gas-liquid bubbly flow in ducts, Chemical Engineering and Processing*, **40,** pp. 437-447, 2001.
[7] J.O. Hinze, *Fundamentals of the hydrodynamic mechanism of splitting in dispersion process*, AIChE Journal, **1,** pp. 289-295, 1955.
[8] Winterton P., Orby P., Bubble size in bubbly flow in ducts and bubble columns, *Proceedings of the 10th International Heat Transfer Conference*, **6,** pp. 295-299, 1994.
[9] Fogg P.T.G., Some Aspects of the Solubility of Gases in Liquids, *Monatshefte für Chemie*, **134,** pp. 619 – 631, 2003.
[10] Jones S.F., Evans G.M., Galvin K.P., The cycle of bubble production from a gas cavity in a supersaturated solution, *Advances in Colloid and Interface Science*, **80,** pp. 27-50, 1999a.
[11] Lubetkin. S., Blackwell M., The nucleation of bubbles in supersaturated solutions, *Journal of Colloid and Interface Science*, **26,** pp. 610-615, 1988.
[12] Winterton R.H.S., Sizes of bubbles produced by dissolved gas coming out of solution on the walls of pipes in flowing Systems, *Chemical Engineering Science*, **27,** pp. 1223-1230, 1972a.
[13] Scriven L. E., On the dynamics of phase growth, *Chemical Engineering Sciences*, **10,** pp. 1-13, 1958.
[14] Al-Hayes R.A.M., Winterton R.H.S., Bubble growth in flowing liquids, *International Journal of Heat and Mass Transfer*, **24,** pp. 213-221, 1981a.
[15] Al-Hayes R.A.M., Winterton R.H.S., Bubble diameter on detachment in flowing liquids, *International Journal of Heat and Mass Transfer*, **24,** pp. 223-229, 1981b.
[16] Hepworth N.J., Boyd J.W.R., Hammod J.R.M., Varley J., Modelling the effect of liquid notion on bubble nucleation during beer dispense, *Chemical Engineering Science*, **58,** pp. 4071-4084, 2003.
[17] Prodanovic V., Fraser D., Salcudean M., Bubble behaviour in sub cooled flow boiling of water at low pressures and low flow rates, *International Journal of Multiphase Flow*, **28,** pp. 1-19, 2001.
[18] Image-Pro Plus, *Start-Up Guide*, Media Cybernetics, 2010.
[19] Coleman, H.W., Steele, W.G., *Experimentation and uncertainty analysis for engineers*, 2nd ed., John Wiley& Sons Inc., New York, 1999.
[20] Abdelmessih A.H., Hooper F.C., Nangia S., Flow effects on bubble growth and collapse in surface boiling, *International Journal for Heat and Mass Transfer*, **15,** pp. 115-125, 1972.
[21] Verschaeren R., *Degassing nucleation sites in water flow under practical heating conditions*, Master in Mechanical Engineering, Technical University Eindhoven, 2010.